ASTRONOMY & ASTROPHYSICS
SUPPLEMENT SERIES

Astron. Astrophys. Suppl. Ser. **131**, 435–449 (1998)

A new sample of faint Gigahertz Peaked Spectrum radio sources

I.A.G. Snellen[1,2], **R.T. Schilizzi**[1,3], **A.G. de Bruyn**[4,5], **G.K. Miley**[1], **R.B. Rengelink**[1], **H.J. Röttgering**[1], **and M.N. Bremer**[1,6]

[1] Leiden Observatory, P.O. Box 9513, 2300 RA, Leiden, The Netherlands
[2] Institute of Astronomy, Madingley Road, Cambridge CB3 0HA, UK
[3] Joint Institute for VLBI in Europe, Postbus 2, 7990 AA, Dwingeloo The Netherlands
[4] Netherlands Foundation for Research in Astronomy, Postbus 2, 7990 AA, Dwingeloo, The Netherlands
[5] Kapteyn Institute, Postbus 800, 9700 AV, Groningen, The Netherlands
[6] Institut d'Astrophysique de Paris, 98bis Boulevard Arago, 75014 Paris, France

Received January 21; accepted March 18, 1998

Abstract. The Westerbork Northern Sky Survey (WENSS) has been used to select a sample of Gigahertz Peaked Spectrum (GPS) radio sources at flux densities one to two orders of magnitude lower than bright GPS sources investigated in earlier studies. Sources with inverted spectra at frequencies above 325 MHz have been observed with the WSRT at 1.4 and 5 GHz and with the VLA at 8.6 and 15 GHz to select genuine GPS sources. This has resulted in a sample of 47 GPS sources with peak frequencies ranging from ∼500 MHz to > 15 GHz, and peak flux densities ranging from ∼40 to ∼900 mJy. Counts of GPS sources in our sample as a function of flux density have been compared with counts of large scale sources from WENSS scaled to 2 GHz, the typical peak frequency of our GPS sources. The counts can be made similar if the number of large scale sources at 2 GHz is divided by 250, and their flux densities increase by a factor of 10. On the scenario that all GPS sources evolve into large scale radio sources, these results show that the lifetime of a typical GPS source is ∼250 times shorter than a typical large scale radio source, and that the source luminosity must decrease by a factor of ∼10 in evolving from GPS to large scale radio source. However, we note that the redshift distributions of GPS and large scale radio sources are different and that this hampers a direct and straightforward interpretation of the source counts. Further modeling of radio source evolution combined with cosmological evolution of the radio luminosity function for large sources is required.

Key words: galaxies: active — quasars — radio continuum: galaxies

1. Introduction

Gigahertz Peaked Spectrum (GPS) radio sources are a class of extragalactic radio source characterized by a spectral peak near 1 Gigahertz in frequency (e.g. Spoelstra et al. 1985). The spectral peak in these compact luminous objects is believed to be due to synchrotron self absorption caused by the high density of the synchrotron emitting electrons in the radio source. GPS sources are interesting objects, both as Active Galactic Nuclei (AGN) and as cosmological probes. It has been suggested that they are young radio sources ($< 10^4$ yr) which evolve into large radio sources (Fanti et al. 1995; Readhead et al. 1996; O'Dea & Baum 1997), and studying them would then provide us with important information on the early stages of radio source evolution. Alternatively GPS sources may be compact because a particularly dense environment prevents them from growing larger (e.g. O'Dea et al. 1991).

Important information about the nature of GPS radio sources comes from the properties of their optical counterparts. The galaxies appear to be a homogeneous class of giant ellipticals with old stellar populations (Snellen et al. 1996a,b; O'Dea et al. 1996) and are thus useful probes of galaxy evolution with little or no contamination from the active nucleus in the optical. GPS quasars have a different redshift distribution to their galaxy counterparts ($2 < z < 4$, O'Dea et al. 1991) and their radio

The Westerbork Synthesis Radio telescope (WSRT) is operated by the Netherlands Foundation for Research in Astronomy with financial support from the Netherlands Organisation for Scientific Research (NWO).

The Very Large Array (VLA) is operated by the U.S. National Radio Astronomy Observatory which is operated by the Associated Universities, Inc. under cooperative agreement with the National Science Foundation.

morphologies are also quite unlike those of GPS galaxies. The relationship between GPS quasars and galaxies, if any, remains uncertain (Stanghellini et al. 1996).

Previous work on GPS sources has concentrated on the radio-bright members of the class, with $S_{5\mathrm{GHz}} > 1$ Jy (Fanti et al. 1990; O'Dea et al. 1991; Stanghellini et al. 1996; de Vries et al. 1997). We are carrying out investigations of GPS sources at fainter flux density levels, in order to compare their properties with their radio bright counterparts. This enables us to investigate the properties of GPS sources as a function of radio luminosity, redshift, and rest frame peak frequency. The selection of a sample at intermediate flux densities was described in Snellen et al. (1995a). This paper describes and discusses the selection of an even fainter sample from the Westerbork Northern Sky Survey (WENSS, Rengelink et al. 1997).

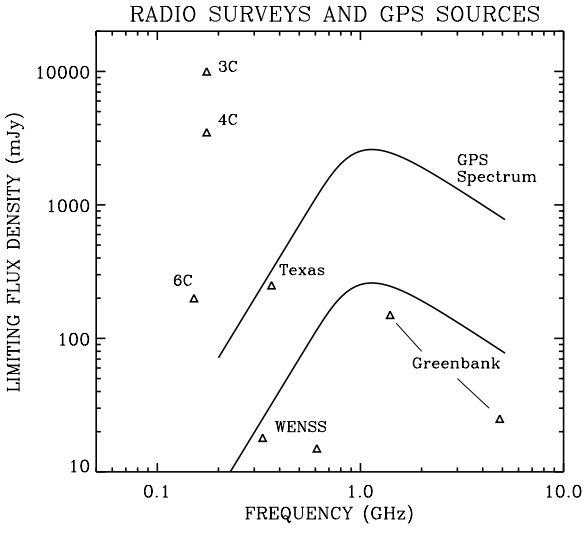

Fig. 1. Overview of the major radio surveys in the northern sky: the Greenbank Surveys (Condon & Broderick 1985; Gregory & Condon 1991), the Texas Survey (Douglas et al. 1996), and the Cambridge 3C, 4C, and 6C surveys. The curves represent the spectra of a homogeneous synchrotron self absorbed radio source, with a peak frequency of 1 GHz and peak flux density of 300 mJy (lower curve) and 3000 mJy (upper curve). Samples of GPS sources can be constructed using WENSS flux density measurements in the optically thick part of their spectra which are more than an order of magnitude fainter than samples selected using the Texas Survey

2. Selection of GPS sources

2.1. The Westerbork Northern Sky Survey

The Westerbork Northern Sky Survey (WENSS) is being carried out at 325 and 609 MHz (92 and 49 cm) with the Westerbork Synthesis Radio Telescope (WSRT). At 325 MHz, WENSS covers the complete sky north of 30° to a limiting flux density of approximately 18 mJy (5σ). At 609 MHz, about a quarter of this area, concentrated at high galactic latitudes, has been surveyed to a limiting flux density of approximately 15 mJy (5σ). The systematic errors in flux density in WENSS were found to be $\sim 5\%$ (Rengelink et al. 1997). The survey was conducted in mosaicing mode which is very efficient in terms of observing time. In this mode, the telescope cycles through 80 evenly spaced field centres, during each of a number of 12^{h} syntheses with different spacings of array elements. The visibilities are sufficiently well sampled for all 80 fields that it is possible to reconstruct the brightness distribution in an area of the sky, ∼100 square degrees, which is many times larger than the primary beam of the WSRT. Individual fields are referred to as *mosaics*, and have a resolution (FWHM of the restoring beam) of $54'' \times 54''$ cosec δ at 325 MHz and $28'' \times 28''$ cosec δ at 609 MHz. From the combined mosaics, maps are made with a uniform sensitivity and regular size, which are called *frames*. The 325 MHz frames are $6° \times 6°$ in size and positioned on a regular $5° \times 5°$ grid over the sky, which coincides with the position grid of the new Palomar Observatory Sky Survey (POSS II, Reid et al. 1991) plates. A detailed description of WENSS is given by Rengelink et al. (1997)

2.2. Selection of a sample of candidate GPS sources

A deep low frequency radio survey such as WENSS is crucial for selecting a sample of faint GPS sources. It is the inverted spectrum at low frequencies which distinguishes them from other types of radio sources. Figure 1 shows the major large-sky radio surveys in the northern sky with theoretical spectra of homogeneous synchrotron self absorbed radio sources (e.g. Moffet 1975) superimposed, which have spectral peak frequencies of 1 GHz. Samples of GPS sources can be constructed using WENSS flux density measurements in the optically thick part of their spectra which are ten times fainter than samples selected using the Texas Survey (Douglas 1996).

When we selected our sample, only a small part of the WENSS region had been observed and the data reduced to the point of providing source lists. The 325 MHz WENSS data used to select GPS sources are from two regions of the sky; one at $15^{\mathrm{h}} < \alpha < 20^{\mathrm{h}}$ and $58° < \delta < 75°$, which is called the *mini-survey* region (Rengelink et al. 1997), and the other at $4^{\mathrm{h}}00^{\mathrm{m}} < \alpha < 8^{\mathrm{h}}30^{\mathrm{m}}$ and $58° < \delta < 75°$, where α is right ascension and δ is declination. These were the first two regions observed, reduced and analysed for WENSS. The mini-survey region, which is roughly centered on the North Ecliptic Pole, was chosen as the first area for analysis because it coincides with the NEP-VLA survey at 1.5 GHz (Kollgaard et al. 1994), the deep 7C North Ecliptic Cap survey (Lacy et al. 1995; Visser et al. 1995), the deepest part of the ROSAT All Sky survey (Bower et al. 1996) and the IRAS survey (Hacking & Houck 1987). The high declination of the two regions is very convenient for VLBI experiments, because their

locations are circumpolar for almost all the major EVN and VLBA radio telescopes. At the time of selection WENSS 609 MHz data was available for only about one third of the mini-survey region. The regions for which both 325 and 609 MHz source lists were available cover 119 square degrees of the sky. The regions for which only 325 MHz data were available cover 216 square degrees in the mini-survey region and 306 square degrees in the other region.

These source lists were correlated with those from the Greenbank 5 GHz (6 cm) survey (Gregory & Condon 1991; Gregory et al. 1996), which has a limiting flux density of 25 mJy (5σ). For the faintest sources the new Greenbank source list (Gregory et al. 1996) was used, which is based on more data. Candidate GPS sources were selected on the basis of a positive spectral index α between 325 MHz and 5 GHz, where the spectral index is defined by $S \sim \nu^{\alpha}$. If 609 MHz data was also available, an "inverted" spectrum between 325 MHz and 609 MHz was used as the selection criterion. This in fact increased the sensitivity of the selection process to GPS sources with low peak frequencies ($<$ 1 GHz). Note that in general for a GPS source, the 325 − 609 MHz spectral index will be more positive than the 325 − 5000 MHz spectral index for a spectral peak in the 1 GHz range. Hence, using the 325 − 609 MHz selection criterion will not miss any GPS sources which would have been found using the 325 − 5000 MHz selection criterion, it will only add extra sources with lower peak frequencies.

In total, 117 inverted spectrum sources were selected; 37 using the 325 − 609 MHz selection and 82 using the 325 − 5000 MHz selection. They are listed in Table 1. Columns 1, and 2 give the name, right ascension and declination (B1950) (obtained from the VLA observations), Cols. 3, 4 and 5 the 325 MHz, 609 MHz and 5 GHz flux densities, and Cols. 6 and 7 give the 325 − 609 MHz and 325 − 5000 MHz spectral indices. The uncertainties in the 325 − 5000 MHz spectral indices range from 0.03 to 0.05 (for the faintest objects), and the uncertainties in the 325 − 609 MHz spectral index range from 0.10 to 0.40.

2.3. Additional radio observations

An apparently inverted or peaked spectrum could be caused by variability at any or all of the selection frequencies, due to the fact that the 325, 609 and 5000 MHz surveys were observed at different epochs. The 5 GHz Greenbank survey was made in 1987, while the 325 MHz and 609 MHz data were taken in 1993. To select the genuine GPS sources, additional quasi-simultaneous observations at other frequencies are required to eliminate flat spectrum, variable radio sources. Furthermore, high frequency data is needed to confirm their turnover, and measure the (steep) spectrum in the optically thin part of their spectra. Therefore VLA observations were taken at 8.4 and 15 GHz, and WSRT observations at 1.4 and 5 GHz. Later, after the selection process, data at 1.4 GHz from the NRAO VLA Sky Survey (NVSS, Condon et al. 1996) became available and were used to supplement our spectra.

2.3.1. WSRT observations at 1.4 and 5 GHz

The WSRT was used to observe the candidate GPS sources at 1.4 and 5 GHz. The 1.4 GHz observations were performed on 20 February and 10 March 1994 using 8 bands of 5 MHz between 1377.5 and 1423.5 MHz, providing a total bandwidth of 40 MHz. The sources were all observed for about 100 seconds at two to three different hour angles. This resulted in a noise level of typically 1 mJy/beam and a resolution of $15'' \times 15''\mathrm{cosec}\ \delta$. The results are shown in Col. 8 of Table 1.

In order to improve the 5 GHz Greenbank flux density measurements, observations were carried out with the WSRT at 4.87 GHz on May 15 1994 using a bandwidth of 80 MHz, at a time when the WSRT was participating a VLBI session. Unfortunately only three telescopes were equipped with 5 GHz receivers. Only sources between 4 and 8 hours right ascension were observed, and the uncertainty in the measured flux densities is large ($\sim$ 15%). The resulting flux densities are listed in Col. 13 in Table 1.

2.3.2. VLA Observations at 8.4 and 15 GHz

The candidate GPS sources were observed with the VLA in B-configuration at 8.4 and 15 GHz on 23 July 1994. At both frequencies, the objects were observed in a standard way using a bandwidth of 2×25 MHz. The phases were calibrated using standard nearby VLA phase calibrators. Total integration times were typically 100 seconds at both frequencies, resulting in noise levels of 0.2 and 1.0 mJy/beam respectively. Systematic errors in flux density of VLA observations at these frequencies are typically about 3% (e.g. Carilli et al. 1991). The data were reduced using AIPS in a standard manner, including several iterations of phase self-calibration. The synthesized beams have half widths of $1.5'' \times 0.8''$ and $0.8'' \times 0.5''$ at 8.4 and 15 GHz respectively. Several candidate GPS sources had already been observed at 8.4 GHz on February 26 1994 and April 3 1994 during the Cosmic Lens All Sky Survey (CLASS) program (e.g. Myers et al. 1995); these were not re-observed by us at 8.4 GHz. The CLASS 8.4 GHz observations were made using the VLA in A configuration in a standard way, also with a bandwidth of 2×25 MHz and an average integration time of 30 seconds. The resolution of the CLASS observations was $\sim 0.2''$, and the noise level $\sim$ 0.4 mJy/beam.

The results of the VLA observations are listed in Cols. 9 and 10 in Table 1. All of the sources were unresolved, except for B1608+6540, which was found to be

Table 1. The sample of candidate GPS sources. Column 1 gives the B1950 source name, Col. 2 the VLA position, Cols. 3, 4 and 5 the flux densities from WENSS at 325 and 609 MHz and of the Greenbank Survey at 5 GHz. Columns 6 and 7 give the 325 − 609 MHz and the 325 − 5000 MHz spectral indices, Cols. 8, 9 and 10 the flux densities from the WSRT at 1.4 GHz, and from the VLA at 8.4 and 15 GHz. A cross in Col. 11 indicates whether the source was selected in the final sample. Columns 12, 13 and 14 give the NVSS 1.4 GHz, the WSRT 5 GHz and the MERLIN 5 GHz flux densities

Source	R.A.(1950)			Decl.(1950)			S_{325}	S_{609}	$S_{5.0}^{\rm gb}$	α_{609}^{325}	α_{5000}^{325}	$S_{1.4}^{\rm wsrt}$	$S_{8.6}^{\rm VLA}$	$S_{14.9}^{\rm VLA}$	GPS	$S_{1.4}^{\rm nvss}$	$S_{5.0}^{\rm wsrt}$	$S_{5.0}^{\rm merlin}$
	h	m	s	°	′	″	(mJy)	(mJy)	(mJy)			(mJy)	(mJy)	(mJy)		(mJy)	(mJy)	(mJy)
B0400+6042	4	0	7.22	60	42	29.0	81		100		+0.08	180	85	36	+	166	73	85
B0402+6442	4	2	56.73	64	42	52.4	48		69		+0.13	63	56	45		70	32	
B0406+7413	4	6	37.39	74	13	22.5	63		66		+0.02	56	54	36		60	49	
B0418+6724	4	18	50.86	67	24	7.2	47		95		+0.26	54	96	79		50	46	
B0436+6152	4	36	15.80	61	52	10.0	70		127		+0.22	208	108	60	+	238	101	122
B0441+5757	4	41	53.90	57	57	21.7	60		115		+0.24	95	128	96	+	91	91	101
B0456+7124	4	56	0.15	71	24	10.1	88		148		+0.19	121	213	216		116	181	
B0507+6840	5	7	4.48	68	40	44.7	27		33		+0.07	30	41	29		31	28	
B0513+7129	5	13	38.82	71	29	55.1	121		181		+0.15	236	96	60	+	244	123	131
B0515+6129	5	15	19.62	61	28	59.3	40		45		+0.04	26	62	41		28	43	
B0518+6004	5	18	42.78	60	4	55.9	88		113		+0.09	67	92	102		101	56	
B0531+6121	5	31	55.43	61	21	31.0	18		38		+0.27	19	44	23	+	22	33	23
B0535+6743	5	35	57.15	67	43	49.8	83		182		+0.29	97	235	136	+	148	177	168
B0536+5822	5	36	8.26	58	22	3.8	26		27		+0.01	36	54	39		31	37	
B0537+6444	5	37	15.12	64	45	3.7	18		32		+0.21	29	17	9	+	28	17	17
B0538+7131	5	38	38.30	71	31	20.9	19		77		+0.51	45	68	29	+	48	90	73
B0539+6200	5	39	54.51	62	0	2.2	47		104		+0.29	123	80	66	+	126	112	99
B0542+7358	5	42	50.98?	73	58	32.5	29		29		+0.00	46	33	24		44	34	
B0543+6523	5	43	40.36	65	23	24.6	26		43		+0.18	65	47	27	+	72	49	43
B0544+5847	5	44	3.18	58	46	55.8	33		42		+0.09	67	43	22	+	60	48	34
B0552+6017	5	52	35.07	60	17	30.1	15		26		+0.28	44	11	< 3	+	47	11	13
B0556+6622	5	56	13.00	66	22	57.7	22		25		+0.05	12	30	20		24	27	
B0557+5717	5	57	31.76	57	17	19.7	19		29		+0.16	63	28	14	+	69	36	30
B0601+7242	6	1	57.83	72	42	54.6	16		26		+0.18	14	18	8		14	37	
B0601+5753	6	1	22.05	57	53	31.8	19		162		+0.83	141	149	138	+		207	192
B0605+7218	6	5	6.15	72	18	51.1	24		116		+0.51	80	39	60		60	65	
B0607+7335	6	7	33.86	73	35	53.0	20		54		+0.36	73	86	54		53	87	
B0607+7107	6	7	54.42	71	8	14.1	21		25		+0.10	24	21	18		27	42	
B0609+7259	6	9	14.93	72	59	50.7	20		25		+0.08	16	16	11		22	23	
B0738+7043	7	38	37.86	70	43	9.2	47		84		+0.19	34	18	106		73	100	
B0741+7213	7	41	30.37	72	12	58.5	65		106		+0.18	96	54	55		99	75	
B0748+6343	7	48	27.42	63	43	31.7	24		54		+0.42	39	69	85	+	44	87	130
B0752+6355	7	52	21.41	63	55	59.5	15		254		+1.04	133	298	282	+	196	376	303
B0755+6354	7	55	20.66	63	54	25.4	25		38		+0.15	26	17	18	+	26	21	19
B0756+6647	7	56	47.89	66	47	27.8	44		164		+0.48	90	80	77	+	104	109	97
B0758+5929	7	58	13.00	59	29	56.9	97		178		+0.22	203	127	101	+	207	185	163
B0759+6557	7	59	12.95	65	57	45.9	15		27		+0.22	40	14	8	+	48	26	21
B0800+6754	8	0	6.92	67	54	31.9	78		78		+0.00	30	33	32		39	38	
B0802+7323	8	2	32.27	73	23	53.3	318		321		+0.00	277	387	445		307	437	
B0808+6518	8	8	5.14	65	18	10.8	35		42		+0.07	52	17	21		31	32	
B0810+6440	8	10	7.59	64	40	29.1	96		193		+0.26	92	132	179		90	133	
B0820+7403	8	20	43.56	74	2	53.8	104		108		+0.01	81	65	63		102	97	
B0824+6446	8	24	31.62	64	46	27.4	24		35		+0.14	30	11	13		44	29	
B0826+7045	8	26	52.55	70	45	44.1	34		109		+0.43	73	63	56	+	79	99	92
B0827+6231	8	27	3.37	62	31	45.9	28		28		+0.00	32	25	33		34	32	
B0828+5756	8	28	33.49	57	56	5.6	29		32		+0.04	37	27	26		53	40	
B0828+7307	8	28	49.08	73	6	58.7	81		104		+0.09	68	58	68		102	86	
B0830+5813	8	30	12.71	58	13	38.8	39		65		+0.29	65	31	23	+	59	43	38
B0830+6300	8	30	37.77	63	0	8.1	26		36		+0.12	54	50	54		62	65	
B0830+6845	8	30	59.69	68	45	33.1	53		74		+0.12	83	136	124		86	159	
B1525+6801	15	25	21.12	68	1	48.9	90		103		+0.05	153	54	29	+	161		91
B1529+6741	15	29	17.85	67	41	58.6	47		55		+0.06	19	32	26		35		
B1529+6829	15	29	45.15	68	29	9.3	51		51		+0.00	29	21	23		27		
B1536+6202	15	36	54.56	62	2	56.4	16		30		+0.23	15	34	24		22		
B1538+5920	15	38	27.46	59	20	39.0	29		73		+0.34	47	36	23	+	45		45
B1539+6156	15	39	32.28	61	56	1.9	34		40		+0.06	15	54	36		33		
B1542+6139	15	42	5.03	61	39	20.9	60		129		+0.28	86	114	119		90		
B1542+6631	15	42	54.19	66	31	18.2	54		86		+0.17	44	81	84		51		
B1550+5815	15	50	55.59	58	15	37.5	86		362		+0.53	157	214	212	+			237
B1551+6822	15	51	53.07	68	22	38.7	23		34		+0.14	49	26	10	+	55		27

Table 1. continued

Source	R.A.(1950)			Decl.(1950)			S_{325}	S_{609}	$S^{\rm gb}_{5.0}$	α^{325}_{609}	α^{325}_{5000}	$S^{\rm wsrt}_{1.4}$	$S^{\rm VLA}_{8.6}$	$S^{\rm VLA}_{14.9}$	GPS	$S^{\rm nvss}_{1.4}$	$S^{\rm wsrt}_{5.0}$	$S^{\rm merlin}_{5.0}$
	h	m	s	°	′	″	(mJy)	(mJy)	(mJy)			(mJy)	(mJy)	(mJy)		(mJy)	(mJy)	(mJy)
B1557+6220	15	57	8.43	62	20	7.4	23		37		+0.17	40	12	4	+	42		18
B1559+5715	15	59	5.07	57	15	19.2	27		47		+0.20	55	36	39		68		
B1600+5714	16	0	8.62	57	14	18.8	29		45		+0.16	24	12	76		41		
B1600+7131	16	0	57.00	71	31	40.2	26		103		+0.50	311	37	15	+	308		85
B1604+5939	16	4	56.32	59	39	43.7	71		110		+0.16	111	130	112				
B1607+6026	16	7	30.32	60	26	34.6	79		79		+0.00	16	31	22		34		
B1608+6540	16	8	50.55	65	40	15.1	66		90		+0.11	63	40	78		68		
B1616+6428	16	16	26.42	64	28	7.7	19	37	62	+1.06	+0.43	64	58	58		61		
B1620+6406	16	20	46.19	64	6	12.6	27	30	25	+0.16	−0.03	41	6	< 3	+	43		11
B1622+6630	16	22	50.52	66	30	52.6	23	61	517	+1.55	+1.14	178	230	176	+	159		230
B1623+6859	16	23	36.01	68	59	46.0	32	32	< 25	+0.00		11	3	< 3		18		
B1624+6622	16	24	7.26	66	22	6.7	38	42	< 25	+0.16		33	4	< 3		26		
B1633+6506	16	33	7.49	65	6	52.4	48	66	114	+0.51	+0.30	111	97	90		95		
B1639+6711	16	39	10.76	67	11	47.2	34	61	30	+0.93	−0.05	54	27	19	+	76		40
B1642+6701	16	42	16.42	67	1	22.6	124	126	65	+0.02	−0.24	121	43	24	+	126		56
B1645+6738	16	45	38.00	67	38	0.8	22	22	< 25	+0.00		28	8	5		28		
B1647+6225	16	47	31.26	62	25	49.7	31	59	33	+1.02	+0.02	69	13	3	+	56		17
B1655+6446	16	55	21.09	64	46	21.2	23	52	34	+1.30	+0.14	68	16	9	+	61		23
B1657+5826	16	57	15.96	58	26	31.5	56	63	17	+0.19	−0.44	44	18	13	+	48		23
B1711+6031	17	11	39.99	60	31	45.3	15	29	< 25	+1.05		17	3	< 3		19		
B1712+6727	17	12	50.73	67	27	10.2	28	30	< 25	+0.11		28	23	13		31		
B1714+5819	17	14	56.27	58	19	16.2	21	35	< 25	+0.81		25	6	3		28		
B1718+6024	17	18	18.75	60	24	11.7	19	29	< 25	+0.67		20	3	< 3		18		
B1730+6027	17	30	15.71	60	27	24.9	41	83	34	+1.12	−0.13	178	103	89		161		
B1746+6921	17	46	53.21	69	21	33.5	65	96	144	+0.62	+0.31	161	127	100	+	154		139
B1749+6919	17	49	31.62	69	19	41.3	21	31	18	+0.62	−0.06	27	10	7		32		
B1755+6905	17	55	42.48	69	5	48.4	16	72	77	+2.40	+0.28	84	51	48		78		
B1807+5959	18	7	17.36	59	59	26.5	16	43	30	+1.52	+0.28	47	37	22	+	42		38
B1807+6742	18	7	23.43	67	42	22.3	29	52	< 25	+0.93		47	12	8	+	43		20
B1808+6813	18	8	25.41	68	13	36.1	33	37	24	+0.18	+0.04	42	11	8	+	42		19
B1818+6445	18	18	24.79	64	45	17.1	35	38	< 25	+0.13		24	27	< 3		27		
B1818+6249	18	18	50.02	62	49	56.2	41	50	< 25	+0.32		34	8	6		33		
B1819+6707	18	19	48.42	67	7	20.8	265	330	154	+0.35	−0.20	297	93	68	+	311		142
B1821+6251	18	21	20.03	62	51	52.6	30	38	31	+0.38	+0.01	32	28	19		29		
B1827+6432	18	27	55.40	64	32	13.7	152	228	262	+0.65	+0.20	204	135	120		216		
B1829+6419	18	29	16.62	64	19	23.1	62	95	< 25	+0.68		80	6	4		75		
B1834+6319	18	34	48.26	63	19	49.6	37	46	< 25	+0.35		36	5	< 3		36		
B1838+6239	18	38	12.00	62	39	56.2	15	33	< 25	+1.25		54	7	6		36		
B1841+6715	18	41	7.21	67	15	51.2	36	94	163	+1.53	+0.55	142	98	68	+	178		125
B1841+6343	18	41	18.25	63	43	56.3	15	29	< 25	+1.05		41	10	6		36		
B1843+6305	18	43	6.16	63	5	42.8	15	41	52	+1.67	+0.45	59	27	16	+	81		40
B1850+6447	18	59	27,78	64	47	31.6	49	70	< 25	+0.57		52	6	< 3		55		
B1916+6817	19	16	37.66	68	17	51.6	23	39	< 25	+0.84		20	6	4		26		
B1919+6912	19	19	57.99	69	12	26.2	21	28	18	+0.46	−0.06	16	16	14		15		
B1926+6111	19	26	49.66	61	11	20.9	404		613		+0.15	718	85	678		535		
B1934+7111	19	34	41.81	71	11	10.4	92		108		+0.06	142	119	102		179		
B1938+5824	19	38	50.57	58	24	49.9	24		29		+0.07	34	30	25		21		
B1942+7214	19	42	2.24	72	14	31.9	81		158		+0.24	233	147	110	+	233		183
B1944+6007	19	44	21.42	60	7	40.5	20		79		+0.50	12	62	32		17		
B1945+6024	19	45	24.83	60	24	12.6	25		80		+0.43	55	125	188	+	55		84
B1946+7048	19	46	12.02	70	48	21.6	234		643		+0.37	887	389	268	+	953		574
B1951+6915	19	51	34.02	69	15	6.3	23		32		+0.12	24	40	35		33		
B1951+6453	19	51	42.52	64	53	56.1	111		103		+0.00	89	83	59		88		
B1954+6146	19	54	11.69	61	45	58.1	66		132		+0.25	66	182	152	+	61		153
B1958+6158	19	58	45.58	61	58	27.1	52		140		+0.36	111	96	84	+	129		136
B2006+5916	20	06	52.14	59	16	43.5	30		37		+0.08	36	21	18		30		
B2011+7156	20	11	22.95	71	56	9.4	48		134		+0.38	118	103	102				

a quadruple gravitational lens (Snellen et al. 1995b; Myers et al. 1995; Fassnacht et al. 1996)

2.3.3. The NRAO VLA Sky Survey at 1.4 GHz

Observations for the 1.4 GHz NRAO VLA Sky Survey (NVSS, Condon et al. 1996) began in September 1993 and are planned to cover the sky north of declination -40° (82% of the celestial sphere). Data in our regions of interest were taken on 1 November 1993 for the region $4^{\rm h}00^{\rm m} <$ R.A. $< 8^{\rm h}00^{\rm m}$, and on 2 April 1995 for the region between $15^{\rm h}00^{\rm m} <$ R.A. $< 20^{\rm h}00^{\rm m}$. The noise level in an image is typically 0.5 mJy/beam and the resolution is $45''$.

2.3.4. MERLIN Observations at 5 GHz

The final sample of genuine GPS sources, as selected in Sect. 2.4, was observed with MERLIN at 5 GHz on 15 and 16 May 1995 during our global VLBI measurements. The sources were observed in three to four "snapshots" of 13 minutes each, resulting in a noise level of typically 0.3 mJy/beam, and a resolution of $0.04''$. All the sources were unresolved. The results are listed in Col. 14 of Table 1. Note that these observations were obtained after, and therefore not used for, the final selection.

2.4. Selection of the Genuine GPS sources

The genuine GPS sources were selected using the 325 MHz and, if available, the 609 MHz WENSS data, 1.4 GHz WSRT data, 5 GHz Greenbank data and 8.4 and 15 GHz VLA data. The WSRT 5 GHz data were not used for selection because they were only available for a part of the sample. The NVSS data was not used for selection, being not available at the time of source selection. However, both the 5 GHz WSRT and 1.4 GHz NVSS data were used for variability studies (see Sect. 3).

The selection criteria were as follows:

1. The spectrum must decrease monotonically below the frequency with the highest flux density, taking into account an assumed uncertainty of 10% in flux density.
2. The spectrum must decrease monotonically above the frequency with the highest flux density, taking into account an assumed uncertainty of 10% in flux density.
3. The Full Width Half Maximum (FWHM) defined by the logarithm of the spectrum must be less than 2 decades in frequency. A spectral index of 0.5 is assumed below 325 MHz, and a spectral index of -0.5 above 15 GHz.
4. The Greenbank 5 GHz flux density must be greater than 20 mJy. This allowed imaging of the source with global VLBI at 5 GHz without recourse to phase referencing. Note that if no Greenbank flux density was available (noise level is about 5 mJy), the flux density was estimated by interpolating the 1.4 and 8.4 GHz flux density points.

The resulting sample of 47 sources is listed in Table 2. One of the sources, B1807+5959, did not obey the criterion of decreasing flux density above the peak frequency, because the 5 GHz Greenbank flux density flux point is too low. However it was kept in the sample because the fall off in flux density at both low and high frequencies suggests that the low flux density point at 5 GHz is due to the different epoch of the Greenbank observations. Additional observations showed this to be true.

The spectra of the selected GPS sources were fitted with the following function

$$S(\nu) = S_{\rm max}/(1-{\rm e}^{-1}) \times \left(\frac{\nu}{\nu_{\rm max}}\right)^{k} \times (1-{\rm e}^{-\left(\frac{\nu}{\nu_{\rm max}}\right)^{l-k}}) \quad (1)$$

where k is the optically thick spectral index, l the optically thin spectral index, and $S_{\rm max}$ and $\nu_{\rm max}$ respectively the peak flux density and peak frequency. This equation, which represents a homogeneous synchrotron self absorbed radio source for $k = 2.5$ (e.g. Moffet 1975), fits the spectral peak well in most cases, however it did not always fit the flux density points at the lowest and highest frequency frequency adequately, and therefore was only used to determine the peak flux density, peak frequency and Full Width Half Maximum of the spectra. The optically thick and thin spectral indices have been determined from the two lowest and the two highest frequency data points respectively. The fitted spectra are shown in Fig. 2. Table 2 gives the characteristics of the GPS sources: Col. 1 gives the source name, Cols. 2 and 3 the peak frequency and peak flux density, Cols. 4 and 5 the optically thick and optically thin spectral indices, and Col. 6 the FWHM of the spectrum in logarithmic units.

Figure 2 shows that three of the 47 sources initially selected probably do not have genuine GPS spectra, namely B0531+6121, B0748+6343 and B0755+6354. In these cases differences between MERLIN, Greenbank and WSRT 5 GHz flux density measurements suggest that the measured spectra are contaminated by flux density variability and it is not clear whether the spectra do indeed exhibit a peak. Although we have included them in the sample, we omit them from the analysis below. Note that no sign of a turnover is seen in B1945+6024, and that there are some sources in the sample which do not have a "clean" peaked spectrum, like B1954+6146 and B0535+6743. To obtain a better determination of the spectral peak of B1954+6146, the 325 MHz flux density data point is not used to fit the spectrum.

3. Flux variability, confusion and extended emission

The measurements at different epochs at 1.4 GHz (WSRT and NVSS) and at 5 GHz (Greenbank, WSRT and

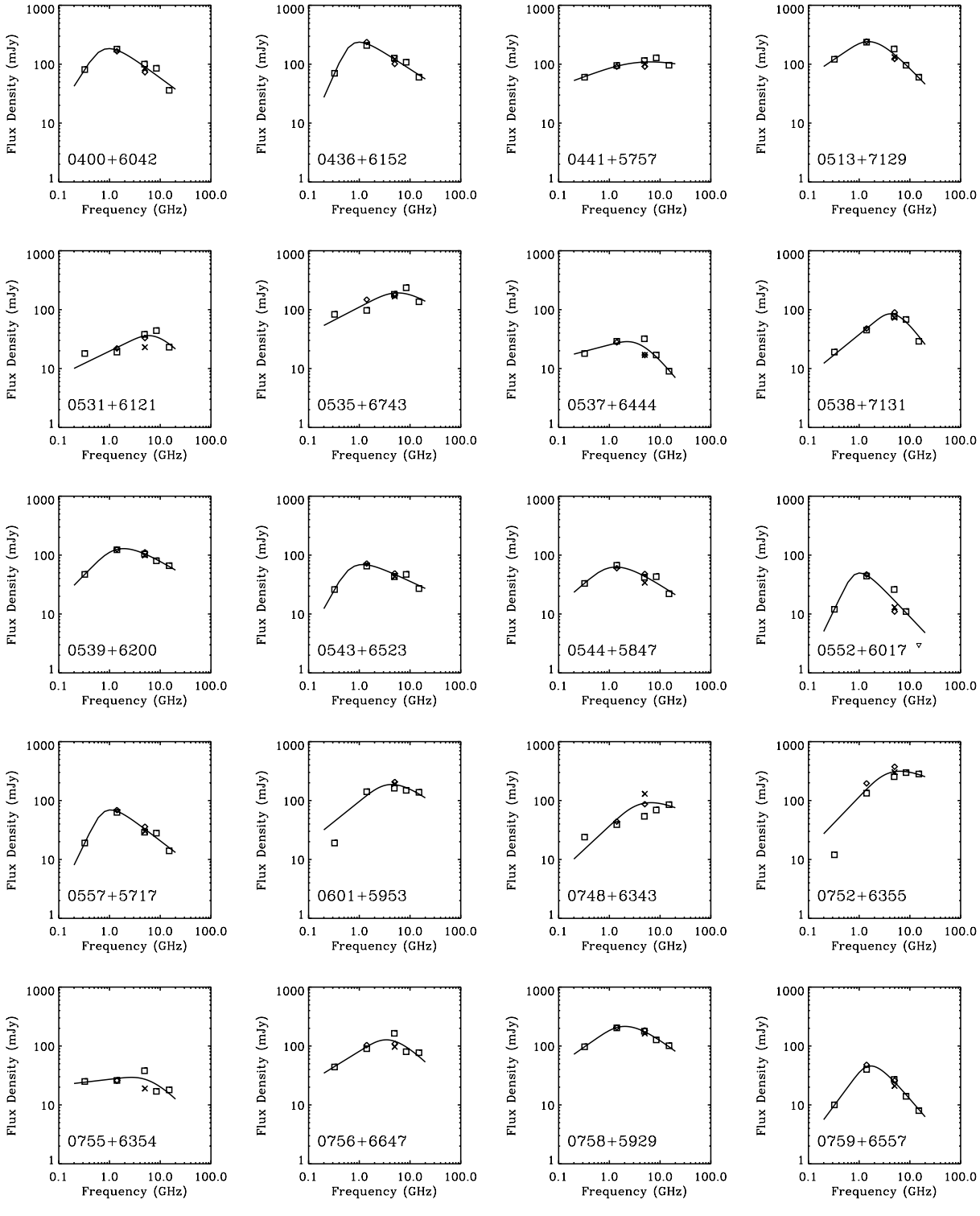

Fig. 2. Radio spectra of individual sources. Crosses indicate MERLIN data, diamonds indicate at 1.4 GHz NVSS data and at 5 GHz WSRT data

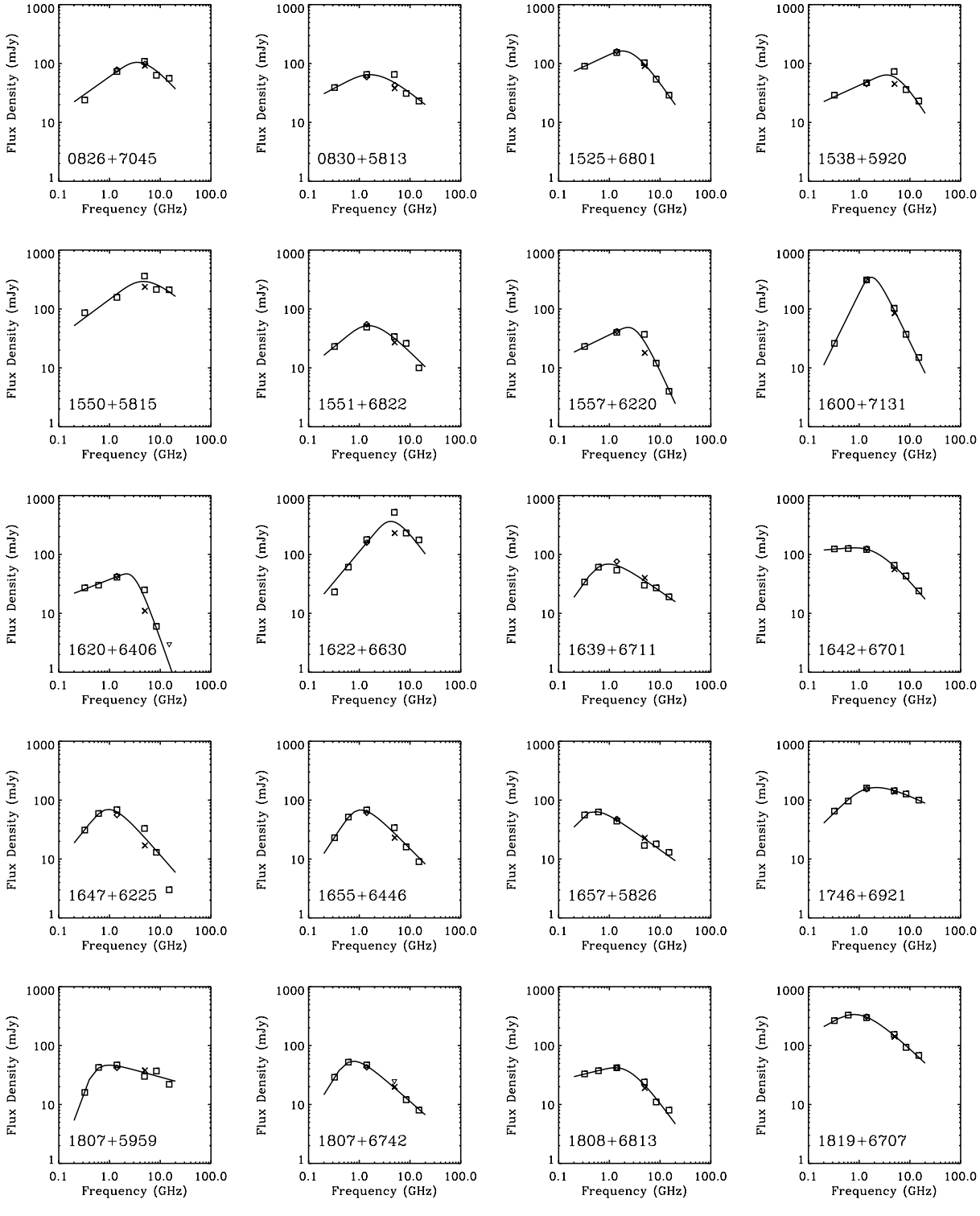

Fig. 2. continued

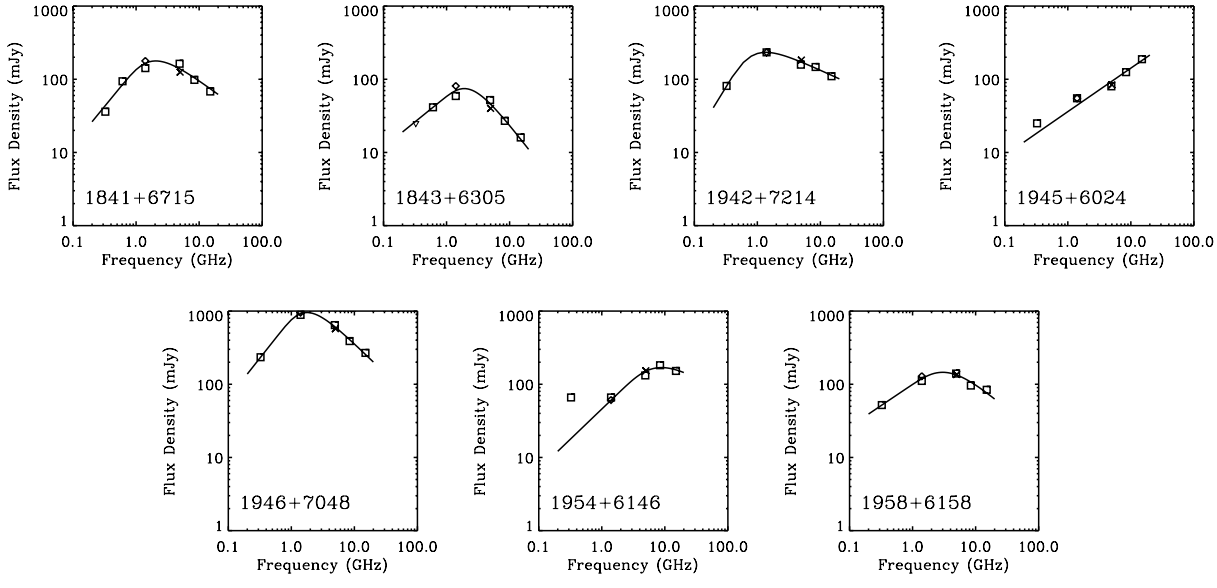

Fig. 2. continued

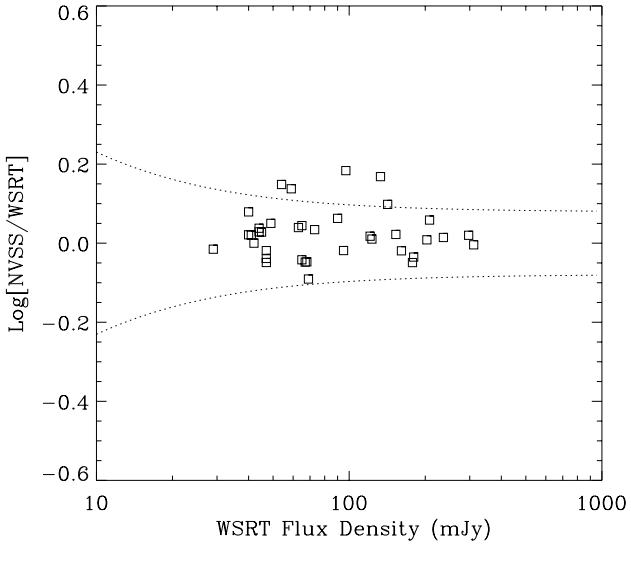

Fig. 3. The logarithm of the ratio between the 1.4 GHz NVSS and WSRT flux densities as function of NVSS flux density for the GPS sources. The dotted lines indicate a difference in flux density of 20% ± 5 mJy

MERLIN) can be used to investigate the variability of the sources in our sample. The measurements are taken with different resolutions, hence if extended emission is present this can contribute to a difference in measured flux densities. In particular at 5 GHz, the Greenbank flux density measurements can be influenced by confusion of background sources in the 3.5′ beam. However, in general this effect is small.

Figure 3 shows the logarithm of the ratio between the 1.4 GHz NVSS and WSRT flux densities as function of WSRT flux density for the GPS sources. Note that for only 5 GPS sources (14%) this difference is larger than 20% ± 5 mJy, which can be caused by either variability or extended emission on scales between 8″ and 35″, or both. For the sources which were not included in the final GPS sample, the "non-GPS sources", the percentage of objects outside 20% ± 5 mJy is 26%. None of the objects with a nearby radio source in the NVSS (see Fig. 4) has a difference between their 1.4 GHz WSRT and NVSS measurements of $> 20\%$. Therefore it seems unlikely that extended emission is causing the discrepancy between the two 1.4 GHz flux density measurements.

Figure 5 shows the logarithm of the ratio of the Greenbank/MERLIN 5 GHz and the WSRT/MERLIN 5 GHz flux density measurements. For 13 out of 43 GPS sources (30%), the Greenbank-MERLIN flux density ratio is greater than 20% + 5 mJy, while none of these ratios are smaller than 20% − 5 mJy. All except two of the WSRT-MERLIN 5 GHz flux density ratios are within 20% ± 5 mJy of each other. In contrast, the WSRT to Greenbank 5 GHz flux densities of 71% of the non-GPS sources differ more than 20%. Hence the candidate GPS sources which turned out not to be GPS sources are clearly more variable than the GPS sources.

The Greenbank flux densities for the GPS sources in our sample are always equal or higher than the MERLIN and WSRT flux densities. This suggests that extended emission or confusion by background sources in the Greenbank measurements plays an important role. Indeed, four of the five sources with nearby components (see Fig. 4) differ in their 5 GHz Greenbank and MERLIN

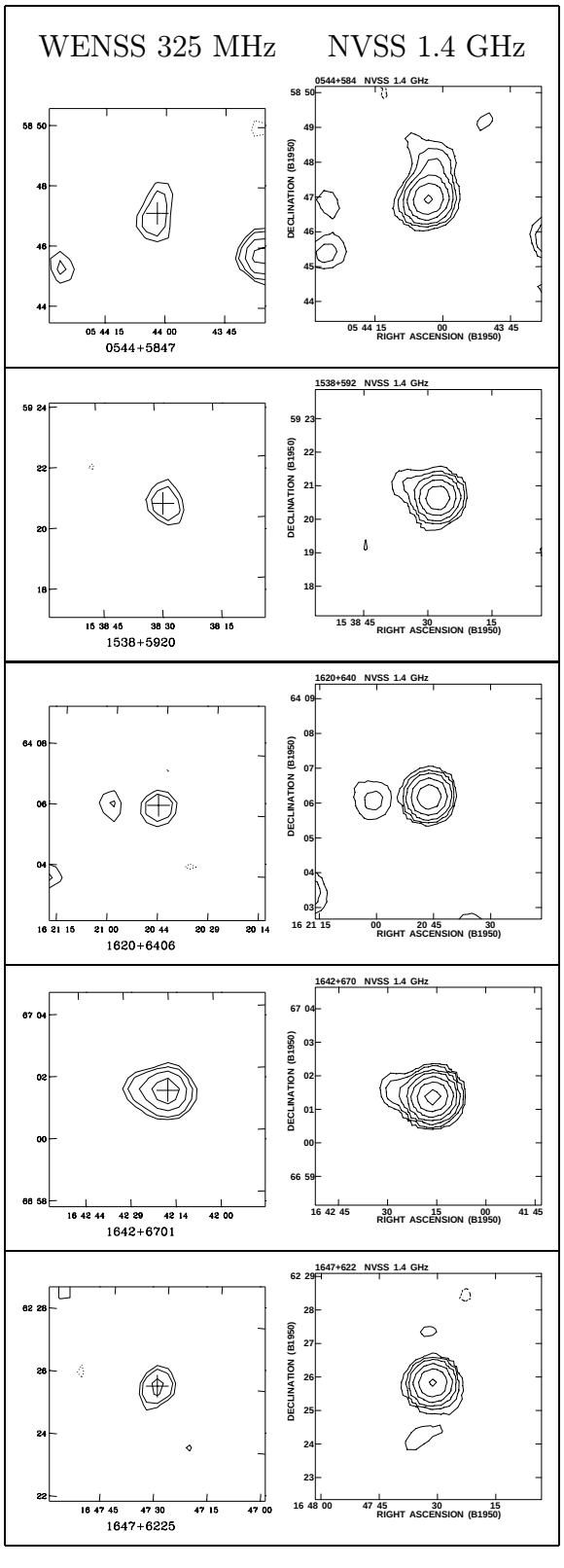

Fig. 4. The WENSS 325 MHz (left) and the NVSS 1.4 GHz (right) maps of the five GPS sources for which nearby radio components are found in the NVSS

Table 2. The resulting sample of GPS sources

GPS Source	$\nu_{\rm max}$ (GHz)	$S_{\rm max}$ (mJy)	$\alpha_{\rm thick}$	$\alpha_{\rm thin}$	$FWHM$ log(freq)
B0400+6042	1.0	184	0.52	−1.48	0.7
B0436+6152	1.0	237	0.79	−1.01	0.7
B0441+5757	6.4	109	0.30	−0.50	1.9
B0513+7129	1.5	242	0.47	−0.81	0.9
B0531+6121	5.9	36	0.09	−1.12	1.0
B0535+6743	5.7	192	0.27	−0.94	1.1
B0537+6444	2.3	29	0.31	−1.10	1.7
B0538+7131	4.2	85	0.61	−1.47	0.7
B0539+6200	1.9	129	0.67	−0.33	0.9
B0543+6523	1.2	69	0.66	−0.96	1.0
B0544+5847	1.4	63	0.45	−1.16	0.9
B0552+6017	1.0	50	0.91	−1.16	0.5
B0557+5717	1.1	69	0.85	−1.20	0.6
B0601+5753	4.4	187	1.37	−0.13	0.9
B0748+6343	6.6	92	0.37	0.36	1.1
B0752+6355	6.4	314	1.79	−0.10	1.4
B0755+6354	4.2	28	0.03	0.10	2.0
B0756+6647	3.4	127	0.54	−0.07	0.8
B0758+5929	2.0	215	0.51	−0.40	1.0
B0759+6557	1.7	46	1.01	−0.97	0.6
B0826+7045	3.5	105	0.79	−0.20	0.8
B0830+5813	1.6	65	0.32	−0.51	1.1
B1525+6801	1.8	163	0.38	−1.07	1.0
B1538+5920	3.5	64	0.32	−0.77	1.0
B1550+5815	4.6	293	0.41	−0.02	0.9
B1551+6822	1.5	52	0.56	−1.65	0.8
B1557+6220	2.3	49	0.40	−1.89	0.9
B1600+7131	1.7	346	1.70	−1.56	0.3
B1620+6406	2.2	47	0.17	−1.56	1.0
B1622+6630	4.0	363	1.55	−0.46	0.5
B1639+6711	1.0	68	0.92	−0.61	0.8
B1642+6701	1.3	124	0.02	−1.01	2.0
B1647+6225	0.9	71	1.03	−2.53	0.5
B1655+6446	1.0	69	1.29	−0.99	0.5
B1657+5826	0.5	64	0.19	−0.56	0.7
B1746+6921	2.2	164	0.63	−0.41	1.1
B1807+5959	1.0	47	1.56	−0.90	1.4
B1807+6742	0.8	54	0.94	−0.70	0.6
B1808+6813	1.3	42	0.20	−0.55	1.7
B1819+6707	0.8	338	0.35	−0.54	1.0
B1841+6715	2.1	178	1.53	−0.63	0.8
B1843+6305	1.9	75	1.53	−0.90	0.7
B1942+7214	1.4	233	0.72	−0.50	1.0
B1945+6024	> 15	> 188	0.54	0.70	-
B1946+7048	1.8	929	0.91	−0.64	0.6
B1954+6146	8.4	169	0.00	−0.31	1.4
B1958+6158	3.3	142	0.52	−0.23	0.9

measurements by more than 20%. However, the flux densities of the nearby components are relatively low, and therefore variability is more likely to be the dominant factor. The absence of ratios < 0.8 is probably caused by a selection effect. The Greenbank measurements are much older (1987) than all the other measurements. If a GPS source has monotonically increased in flux density between 1987 and the first half of this decade than the Greenbank flux density will be significantly lower than the 5 GHz WSRT and the MERLIN flux density measurements. However the chance that

this source will appear in our sample is then very small, since the spectral index between WENSS and Greenbank is probably not inverted. Furthermore the Greenbank flux density would be too low with respect to the newer WSRT 1.4 GHz and the VLA 8.4 GHz measurements to be included in our sample as a GPS source. If a GPS source is monotonically decreasing with flux density between 1987 and the first half of this decade then there is only a problem if the peak frequency is greater than about 10 GHz, which could make both the Greenbank 5 GHz and the VLA 15 GHz measurement greater than the 8.4 GHz flux density measurement. Thus only sources with stable or decreasing flux densities are likely to be selected in our sample. Examples of GPS sources with decreasing flux densities are B0537+6444, B0552+6017, B0756+6647, B0830+5813 and B1538+5920.

Unlike the NVSS observations, the snapshot WSRT observations are not suitable for mapping possible low level extended emission around the GPS sources, due to the poor UV-coverage of the WSRT observations. The NVSS images have been used to look for extended emission around our GPS sources on scales $< 100''$. Extended emission was detected in 5 of our objects, namely B0544+5846, B1538+5920, B1620+6406, B1642+6701 and B1647+6225. Their corresponding maps are shown in Fig. 4. It is not clear if these additional sources are components associated with the GPS objects or superimposed unrelated sources. From the source density in the NVSS survey, we estimate that there is a $\sim 6\%$ chance of finding a radio source with a flux density of > 5 mJy within a radius of $100''$. Hence in our sample of 47 sources, 3 GPS sources might be expected to have unrelated sources within $100''$, while 5 are found. This is not a significant difference.

4. Source counts

Since the 1960s it has been recognized that counts of radio sources can provide important cosmological information, especially about the evolution of radio sources. Identification and source counts statistics indicated that radio sources were preferentially located in early epochs of the universe (Longair 1966). Recently, several authors (Readhead et al. 1996; Fanti et al. 1995; O'Dea et al. 1997) have shown that if GPS and CSS sources evolve into large scale FRI/FRII radio sources, they must significantly decrease in radio luminosity (a factor 10 to 30) to account for the high number of GPS and CSS sources compared to the number of FRI and FRII radio galaxies. In this section the GPS source counts at faint flux densities derived from our faint sample are constructed and discussed.

To be able to derive the GPS source counts from the sample, the intrinsic distribution of GPS sources with peak frequency and peak flux density has to be determined. The observed distribution of peak flux densities and peak frequencies of the GPS sources in our sample is shown in Fig. 6. The diamonds represent the sources initially selected on the basis of their 325 − 5000 MHz spectral index, the squares represent the sources selected on their 325 − 609 MHz spectral index, while the filled squares represent the sources selected from the 325 − 609 MHz comparison which also would have been in the sample if selected on their 325 − 5000 MHz spectral index. It should be noted that Fig. 6 is the observed distribution, and that the selection criteria are a function of peak frequency, peak flux density, and optically thin and thick spectral indices of the sources, making statistical studies complicated.

Whether a GPS source with a certain peak flux density and peak frequency will appear in our sample depends on its optically thin and thick spectral indices. If the optically thick spectral index is too inverted, the 325 MHz flux density is too low to be in the sample. If the optically thin spectral index is too steep, then the 325 − 5000 MHz spectral index will not be inverted. The range of optically thick and thin spectral indices allowed for a GPS source to appear in the sample is a strong function of peak frequency and peak flux density. To be able to derive the parent distribution of peak flux densities and peak frequencies of GPS sources from the observed distribution in our sample, the fraction of GPS sources selected as a function of peak flux density and peak frequency has to be estimated.

We assume that the peak frequency, peak flux density and the optically thin and thick spectral indices are independent of each other. The intrinsic distribution of optically thin and thick spectral indices have to be determined from their observed distributions. The normalized spectra (in both frequency and flux density) of the sources in our sample are plotted in Fig. 7. The solid line represents the best fit of equation 1 to the data, which gives optically thin and thick spectral indices of -0.75 and $+0.80$ respectively. If we assume the intrinsic or parent spectral index distributions to be Gaussian functions with means and standard deviations of -0.75 and 0.15 (thin) and $+0.80$ and 0.18 (thick), then the observed spectral index distributions are recovered after applying the selection effects to the parent spectral index distributions. Although the outcome of this is not very accurate, this is not too important since our main concern is too show that no significant fraction of GPS sources was missed; sources with highly inverted spectral indices of 2, say, are unlikely to be included unless the peak flux density is high and the peak frequency is low enough. Sufficient numbers of these sources could have an effect on the parameters of the optically thick spectral index distribution.

To obtain an indication of the number of sources with very inverted spectra ($\alpha_{\rm thick} > 1.1$), we looked for highly inverted GPS sources in our sample with peak frequencies lower than 2 GHz and peak flux densities greater than 100 mJy, because these will be the least influenced by

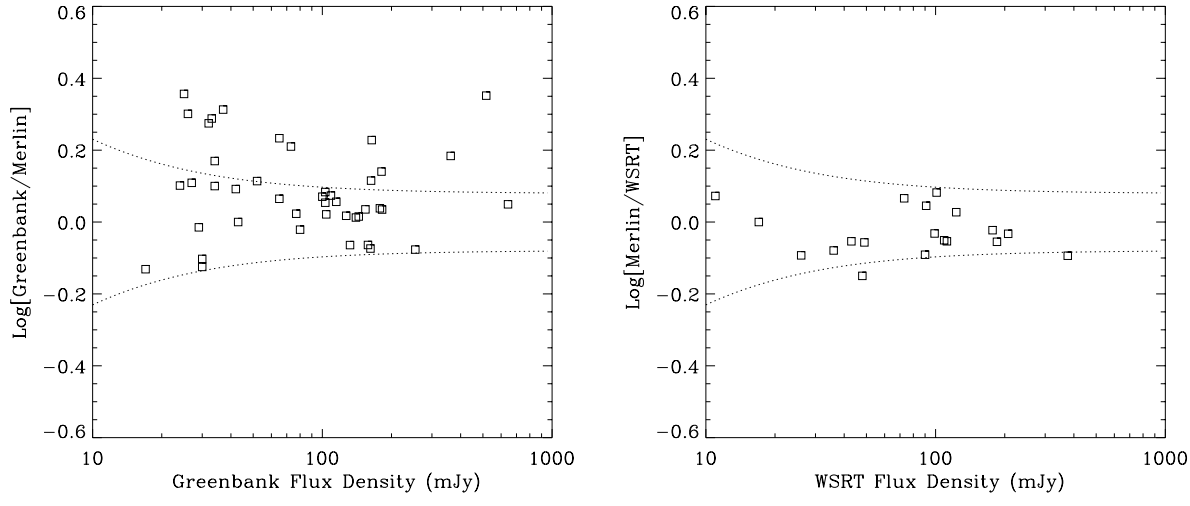

Fig. 5. The logarithm of the ratio of the Greenbank/MERLIN 5 GHz (left) and the WSRT/MERLIN 5 GHz (right) measurements as function of flux density

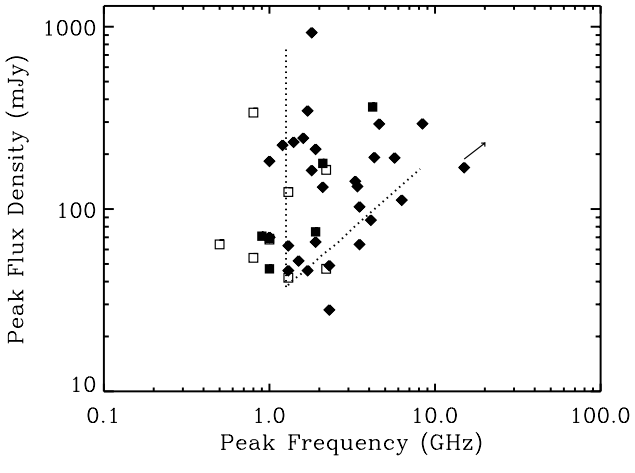

Fig. 6. The distribution of peak frequencies and peak flux densities for the GPS sources in our sample. The diamonds represent the sources selected on their 325 − 5000 MHz spectral index; the squares represent the sources selected on their 325 − 609 MHz spectral index; the filled squares represent the sources selected from the 325 − 609 MHz comparison which also would have been in the sample if selected on their 325 − 5000 MHz spectral index. The dotted lines represent the limits for which a GPS source with optically thin and optical thick spectral indices of −0.75 and +0.80 respectively would be selected on the basis of its 325 − 5000 MHz spectral index. The arrow indicates the lower limit for the peak frequency and peak flux density of B1945+6024

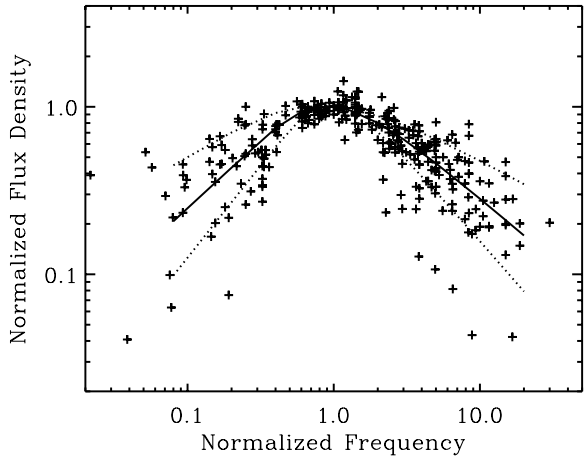

Fig. 7. The spectra of the GPS sources normalized (scaled) in both frequency and flux density. The solid line represents the best fit of equation 1 to the data, which gives optically thick and thin spectral indices of respectively +0.80 and −0.75. The dashed lines represent optical thick and thin spectral indices of +0.5, +1.1, −0.5 and −1.0

selection effects on the optically thick spectral index. Only one object out of ten (10%) was found to have an optically thick spectral index greater than 1.1, while 5% would be expected from the distribution of optically thick spectral indices. Hence we regard any missed population of GPS sources with very steep optically thick spectral indices as small and negligible.

The GPS sources in our sample which have a flux density at 325 MHz $>$ 25 mJy and an inverted spectral index between 325 and 5000 MHz have been used to determine the peak frequency and peak flux density number distributions. The sample is divided into bins of peak flux density of 50 − 100 mJy, 100 − 200 mJy and 200 − 400 mJy and bins of peak frequency of 1 − 2 GHz, 2 − 4 GHz and 4 − 8 GHz. If it is assumed that the parent population of GPS sources has spectral index distributions as

described above, then for each bin the percentage of GPS sources selected in our sample can be determined. For each bin, the number of sources in the parent population of GPS sources was estimated by dividing the number of GPS sources in the sample which fall in the bin by these percentages which were between 40% and 100%.

The observed number of GPS sources, corrected for selection effects as above, have been summed in peak frequency space to determine the surface density of GPS sources as function of flux density. The source counts for the three flux density bins, normalized by the flux density to the power 2.5 are plotted as squares in Fig. 8 (a horizontal relation is expected for a uniformly distributed Euclidean space). The triangles represent the observed surface density counts, not corrected for selection effects, which is a good lower limit. We have used the well defined sample of De Vries et al. (1997) compiled from the working sample of GPS sources from O'Dea et al. (1991) to determine the surface density of GPS sources at high flux density. We determined the number of GPS sources in the de Vries et al. sample which lie within the Pearson and Readhead survey region (Pearson & Readhead 1988, $\delta > 35°$, $|b > 10°|$, 2.0 sr), having peak frequencies between 1 and 8 GHz and flux densities between 2 and 6 Jy. There are five objects satisfying these criteria, which leads to a normalized surface density count of $22 \pm 10\,\mathrm{Jy}^{-3/2}\mathrm{Sr}^{-1}$ in this flux density range, assuming that the spectra of all the radio sources in this region brighter than 2 Jy are well known and that therefore this sample of GPS sources is complete. This measurement is indicated by the diamond symbol in Fig. 8.

Several authors (e.g. Fanti et al. 1995; Readhead et al. 1996; O'Dea et al. 1997) have proposed that GPS sources may evolve into large size FRI/FRII radio sources. Therefore it is interesting to compare the GPS source counts with source counts of FRI/FRII radio sources. It is not very useful to compare them directly to the total radio source counts at comparably high frequency, because these are dominated by compact flat spectrum sources, which are probably not related to GPS sources in an evolutionairy way. However, it can be assumed that the WENSS source counts at 325 MHz are dominated by the large size radio source population, because they have in general steep ($\alpha < -0.5$) spectra. The radio source counts at 325 MHz from the WENSS mini-survey region (Rengelink et al. 1997) is shown in Fig. 8 by the dotted line. Note the resemblance between the shape of this curve and the data for the GPS sources (squares + diamond). The median spectral index is about -0.85, which we used to estimate the source counts for large scale radio sources at higher frequencies comparable to the peak frequencies of the GPS sources. Note that the source counts of the GPS sources are not at a certain fixed frequency, but resemble the distribution of peak flux densities. However, we assume that within the errors the distribution of the peak flux densities of the GPS sources in our sample is the same as for the flux

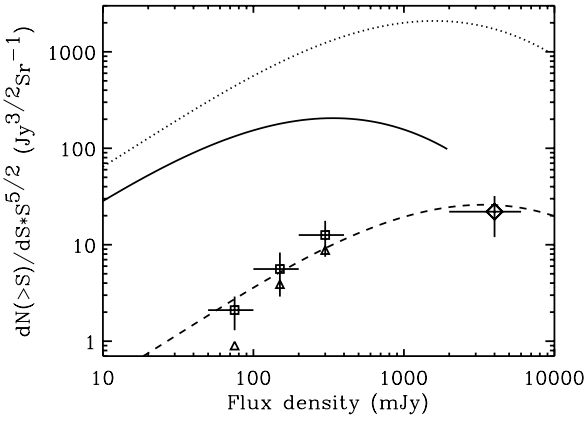

Fig. 8. The number counts of GPS sources as function of peak flux density. The squares are from the data in this paper. The triangles are the observed, not corrected, source counts. The point indicated by the diamond is derived from de Vries et al. (1997). The dotted line represents the WENSS radio source counts at 325 MHz in the mini-survey region, and the solid line are these source counts corrected to 2 GHz using a spectral index of -0.85 (see text). The dashed line is the curve for 1/250 of the 2 GHz counts shifted a factor 10 upward in flux density. This is consistent with the data

densities at the median peak frequency, which is 2 GHz. We determined the large size radio source number counts at 2 GHz from the 325 MHz counts of the WENSS mini-survey region, assuming a fixed spectral index of -0.85. This is represented by the solid curve in Fig. 8.

How can the differences in number counts between the GPS sources and large scale radio sources be interpreted? If GPS sources evolve into large scale radio sources, it is reasonable to assume that they undergo the same cosmological evolution, because the typical lifetime of a radio source is significantly smaller than cosmological timescales. Assuming that the slope of the luminosity function of GPS sources is identical to the slope of the luminosity function of large size radio sources and that *all* GPS sources evolve into large size radio sources, one could obtain the ratio of the life time of the two classes of radio source and the luminosity evolution of the GPS sources. If a radio source is 10 times brighter in its GPS phase than in its FRI/FRII phase, and if the time scale of the GPS phase is 250 times shorter than the age of large scale radio sources, then the dashed line is expected for the source counts of GPS sources. Namely in that case the curve for FRI/FRII radio sources moves a factor 250 down due to the age difference, and a factor of 10 to the right and a factor factor $10^{3/2}$ upward due to the luminosity evolution. This agrees quite well with the observed GPS source counts.

However, this straightforward interpretation is probably too simplistic. Firstly, the redshift distributions of GPS galaxies and large size radio sources are not the

same, which indicates that the slopes of their luminosity functions are different (see Snellen 1997). This has consequences for the interpretation of the radio source counts of GPS sources. It should be investigated if a simple radio source evolution model, as for example presented in Snellen (1997), combined with the cosmological evolution of the radio luminosity function for large size radio sources, is consistent with the GPS source counts presented here. This is beyond the scope of this paper. Secondly, the GPS source counts presented here also include the GPS quasars, although it is not clear that they are related to the GPS galaxies. Excluding the GPS quasars, which contribute about one third of the members of both the bright and faint GPS samples, shifts the squares and the diamond in Fig. 8 down by a factor 1.5. In this case, the number counts are consistent with radio galaxies in the GPS phase being 10 times brighter for a period $\sim$ 400 times shorter than the FRI/FRII phase.

5. Conclusions

A sample of GPS sources has been selected from the Westerbork Northern Sky Survey, with flux densities one to two orders of magnitude lower than bright GPS sources investigated in earlier studies. Sources with inverted spectra at frequencies $>$ 325 MHz have been observed with the WSRT at 1.4 and 5 GHz and with the VLA at 8.6 and 15 GHz to select genuine GPS sources. This has resulted in a sample of 47 GPS sources with peak frequencies ranging from $\sim$500 MHz to $>$ 15 GHz, and peak flux densities ranging from $\sim$40 to $\sim$900 mJy.

Five GPS sources in our sample show extended emission or nearby components in the NVSS maps at 1.4 GHz. However it is not clear if these components are related to the GPS sources.

About 30% of the objects show flux density differences greater than 20% between the Greenbank and MERLIN 5 GHz measurements, with the Greenbank data points all higher than the MERLIN observations. We believe this is due to variability, and that the lack of sources with reverse variability (the MERLIN flux density greater than the Greenbank flux density) is due to a selection effect caused by the "old" epoch (1987) of the Greenbank observations.

GPS source counts are comparable to 1/250 of the 2 GHz source counts for large scale radio sources, if the latter sources were to have 10 times their measured flux densities. Unfortunately, apparent differences in redshift distributions between GPS and large scale radio sources hamper a direct and straightforward interpretation of the source counts. Potentially, the comparison of GPS source counts with that of large scale radio sources can provide clues about the age of GPS sources and their luminosity evolution. If it is assumed that the redshift distributions are the same for GPS and large size radio sources, the source counts indicate that GPS sources have to decrease in luminosity by a factor of $\sim$10 if they all evolve into large scale radio sources.

Acknowledgements. This research was partly supported by the European Commission, TMR Programme, Research Network Contract ERBFMRXCT96-0034 "CERES".

References

Bower R.G., Hasinger G., Castander F.J., Aragon-Salamanca A., Ellis R.S., Gioia I.M., Henry J.P., Burg R., Huchra J.P., Böhringer H., Briel U.G., McLean B., 1996, MNRAS 281, 59

Carilli C.L., Perley R.A., Dreher J.W., Leahy J.P., 1991, ApJ 383, 554

Condon J.J., Broderick J., 1985, AJ 90, 2450

Condon J.J., Cotton W.D., Greisen E.W., Yin Q.F., Perley R.A., Broderick J.J., 1996, in: NCSA Astronomy Digital Image Library, April 1996, p. 1

Douglas J.N., Bash F.N., Bozyan F.A., Torrence G.W., Wolfe C., 1996, AJ 111, 1945

Fanti R., Fanti C., Schilizzi R.T., Spencer R.E., Nan Rendong, Parma P., Van Breugel W.J.M., Venturi T., 1990, A&A 231, 333

Fanti C., Fanti R., Dallacasa D., Schilizzi R.T., Spencer R.E., Stanghellini C., 1995, A&A 302, 317

Fassnacht C.D., Womble D.S., Neugebauer G., Browne I.W.A., Readhead A.C.S., Matthews K., Pearson T.J., 1996, ApJ 460, L103

Gregory P.C., Condon J.J., 1991, ApJS 75, 1011

Gregory P.C., Scott W.K., Douglas K., Condon J.J., 1996, ApJS 103, 427

Hacking P., Houck J.R., 1987, ApJS 63, 311

Kollgaard R.I., Brinkmann W., Chester M.M., Feigelson E.D., Hertz P., Reich P., Wielebinsky R., 1994, ApJS 93, 145

Lacy M., Riley J.M., Waldram E.M., McMahon R.G., Warner P.J., 1995 MNRAS 276, 614

Longair M. 1966, MNRAS 133, 421

Moffet A.T., 1975, in: Stars and Stellar Systems, Vol. IX, Sandage A., Sandage M. and Kristian J. (eds.), p. 211

Myers S.T., Fassnacht C.D., Djorgovski S.G., Blandford R.D., Matthews K., Neugebauer G., Pearson T.J., Readhead A.C.S., Smith J.D., Thompson D.J., Womble D.S., Browne I.W.A., Wilkinson P.N., Nair S., Jackson N., Snellen I.A.G., Miley G.K., de Bruyn A.G., Schilizzi R.T., 1995, ApJS 447, L5

O'Dea C.P., Baum S.A., Stanghellini C., 1991, ApJ 380, 66

O'Dea C.P., Stanghellini C., Baum S.A., Charlot S., 1996, ApJ 470, 806

O'Dea C.P., Baum S.A., 1997, AJ 113, 148

Pearson T.J., Readhead A.C.S., 1988, AJ 328, 114

Readhead A.C.S., Taylor G.B., Xu W., Pearson T.J., Wilkinson P.N., Polatidis A.G., 1996, AJ 460, 612

Reid I.N., Brewer C., Brucato R.J., McKinley W.R., Maury A., Mendenhall D., Mould J.R., Mueller J., Neugebauer G., Phinney J., Sargent W.L.W., Schombert J., Thickstein R., 1991, PASP 103, 661

Rengelink R.B., Tang Y., de Bruyn A.G., Miley G.K., Bremer M.N., Röttgering H.J.A., Bremer M.A.R., 1997, A&AS 124, 259

Snellen I.A.G., Zhang M., Schilizzi R.T., Röttgering H.J.A., de Bruyn A.G., Miley G.K., 1995a, A&A 300, 359

Snellen I.A.G., de Bruyn A.G., Schilizzi R.T., Miley G.K., Myers S.T., 1995b, ApJ 447, L9

Snellen I.A.G., Bremer M.N., Schilizzi R.T., Miley G.K., van Ojik R., 1996a, MNRAS 279, 1294

Snellen I.A.G., Bremer M.N., Schilizzi R.T., Miley G.K., 1996b, MNRAS 283, 123

Snellen I.A.G., PhD thesis 1997, Leiden Observatory, the Netherlands

Spoelstra T.A.T., Patnaik A.R., Gopal Krishna, 1985, A&A 152, 38

Stanghellini C., Dallacasa D., O'Dea C.P., Baum S.A., Fanti R., Fanti C., 1996, in proc of 2nd workshop on GPS&CSS Radio Sources, Snellen I., Schilizzi R.T., Röttgering H.J.A. and Bremer M.N. (eds.), p. 4

Visser A.E., Riley J.M., Röttgering H.J.A., Waldram E.M., 1995, A&AS 110, 419

De Vries W.H., Barthel P.D., O'Dea C.P., 1997, A&A 321, 105